14 Computer Assisted Physics

P. F. Meier, E. Olbrich, S. Pliberšek, S. Renold, J. Schneider, Y. Shen, and E. Stoll
S. Dangel (until Dec. 00) and H.-R. Moser (until June 00)

In this report, we want to concentrate on the following research topics:

- Interpretation of the properties of high temperature superconductivity materials using spin-polarized theoretical methods
- Non-linear dynamical study with particular reference to time series analysis of electroencephalograms

In particular we selectively report on hyperfine interactions at oxygen nuclei in La_2CuO_4 (14.1.1), on the changes in the microscopic structure induced by dopants (14.1.2), and on local distortions in doped La_2CuO_4 (14.1.3). From the collaborations with two groups of the Medical Faculty we present results of a new analysis of sleep electroencephalograms (14.2).

14.1 Electronic structure of high-T_c materials

14.1.1 Transferred hyperfine fields

One explanation of the variant time dependencies of the nuclear–spin-lattice relaxation rates between planar ^{17}O and ^{63}Cu required that the antiferromagnetic fluctuations cancel at the oxygen site. However, this was not in accord with neutron scattering which showed that these fluctuations were incommensurate. This dichotomy led Zha, Barzykin and Pines (ZBP) [1] to propose that the transferred field at the ^{17}O covered an extensive region in the CuO_2 plane which included significant contributions from at least the next nearest neighbour (NNN) copper ions. This would compensate for the non-perfect cancellation of hyperfine field due to the incommensurability and thus reconcile the NMR and neutron scattering data.

It is not obvious how to test the ZBP proposition experimentally so we embarked on a project using our cluster models to see if we could confirm, or otherwise, the proposition. A whole range of clusters for simulation of the La_2CuO_4 system were studied so that the variation of the Fermi contact term D(^{17}O) could be analyzed in terms of the number $n_{\rm NN}$ of nearest neighbours (NN), and the number $n_{\rm NNN}$, of next nearest neighbours. The simplest relation we could conceivably use is of the form

$$D(^{17}\mathrm{O}) = c\ n_{\rm NN} + c'\ n_{\rm NNN}. \tag{14.1}$$

This was found to be quite adequate with the added significance that $c' \approx 0$ as can be seen in Fig. 14.1 where $D(^{17}O)$ is plotted versus $n_{\rm NNN}$ for fixed $n_{\rm NN} = 2$. This implies that

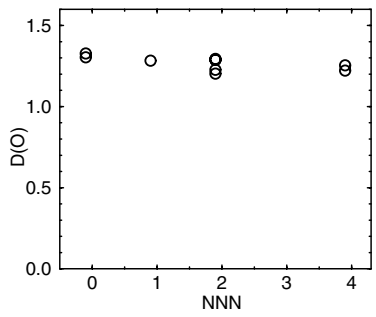

Figure 14.1: *Isotropic contact density at a planar oxygen nucleus as a function of the number of next nearest neighbor copper ions.*

there is no evidence for transferred hyperfine fields on the planar ^{17}O from the next nearest neighbour copper ions. This work does not support the ZBP proposal. It is possible that the dichotomy may be simply due to the difference in detection frequency of the NMR and neutron scattering experiments.

14.1.2 Influence of dopants on the electronic structure of high-T_c materials

Pure La_2CuO_4 is an insulator which becomes metallic and superconducting at low temperatures only by doping, either with excess oxygen or replacing some of the tri-valent lanthanum with bi-valent ions, such as Sr^{2+}.

The role of dopants in high T_c superconductors is generally seen as being limited to the introduction of hole carriers into the CuO_2 plane. This simplified assumption is partly driven by the lack of information on the local atomic and electronic structure around dopants. While experimental evidence favoring inhomogeneous charge distributions of the doped holes is still mounting, the role that dopants play in determining this inhomogeneous ground state, if any, is still unclear.

Conventional band structure calculations are not readily adaptable to studying disrupted periodic structures whereas such cases are more ideally suited for the cluster model. Therefore we can build on the confidence already established with La_2CuO_4.

Previous work [2] has shown that the cluster model gives results for the electric field gradient, on-site and transferred fields for La_2CuO_4 which compare favourably with NMR experimental data. These more recent examples of the extensive studies carried out on La_2CuO_4 continue to demonstrate why we have increasing confidence in the applicability of the cluster method to model copper oxide high-T_c materials. The natural next step was to begin a study of the the effects of doping. The idea that the dopant ions could cause a significant change in the local electronic structure of superconducting cuprates was first introduced in Ref. [4] where it was shown that the important changes in the local molecular orbitals (MOs) as induced by the dopant strontium or interstitial oxygen ions are reflected in the electric field gradient on the neighboring copper nuclei site. This enabled us to resolve a long-standing controversy concerning the interpretation of the nuclear quadrupole resonance spectra in doped La_2CuO_4 on which we briefly reported last year.

With cluster calculations, strontium doping is easily achieved since Sr^{2+} ions substitute some La^{3+} ions unambiguously (see Fig. 14.2) and in the following we compare the results obtained for the undoped system (same cluster as in Fig. 14.2 but with La instead of Sr) and the doped system.

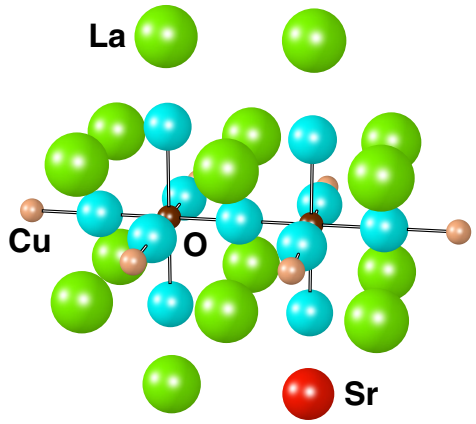

Figure 14.2: *The Cu_2O_{11}/Cu_6SrLa_{15} cluster. For the two central copper atoms (dark) and for the 11 oxygen atoms an all-electron calculation was performed. For the other 6 Cu (bright), Sr and 15 La atoms pseudo-potentials are used.*

For both clusters, the lowest unoccupied molecular orbital (LUMO) is an anti-bonding combination of atomic orbitals with $3d_{x^2-y^2}$ on the copper atoms and $2p_\sigma$ on the oxygens. Of particular interest are the changes in the relative energy differences of the occupied molecular orbitals dominated by the copper d_{zx}, d_{yz}, and d_{xy} orbitals. Some of these calculated MOs are given diagrammatically in Fig. 14.3, where $\Delta E_{0,n}$ denotes the energy difference between the LUMO and the particular n^{th} MO.

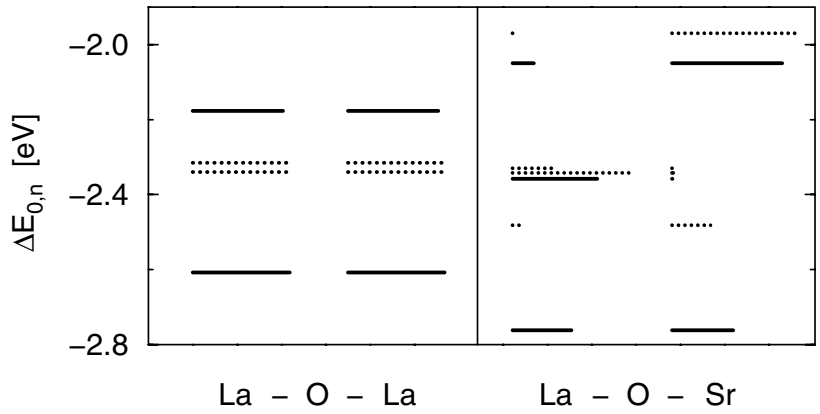

Figure 14.3: *Energy differences between the LUMO and the highest occupied MOs in the clusters described in Fig. 14.1 with contributions from atomic $3d_{zx}$ orbitals (solid bars) and $3d_{yz}$ orbitals (dashed bars). The length of the bar is proportional to the square of the expansion coefficient of the MO into the corresponding atomic orbitals.*

In the left panel the MOs are equally shared by the two Cu atoms as required by symmetry. There are two orbitals for each zx and yz symmetry because there are two Cu atoms. Note that both are anti-bonding linear combinations with O atomic orbitals. The bonding orbitals are deeper in energy and are not shown here. There is a considerable split in energy for the $3d_{zx}$ orbitals and the $3d_{yz}$ orbitals in the right panel of the figure where the symmetry is broken due to the presence of the Sr^{2+}. Since the d_{yz} orbital pair behaves qualitatively in the same way as the d_{zx} orbital pair we will concentrate on the d_{zx} orbital pair only. The one of *lower* energy is largely confined to the left site as shown in Fig. 14.4b whereas the *higher* energy one is localized on the right site as shown in Fig. 14.4c. This is not surprising and a

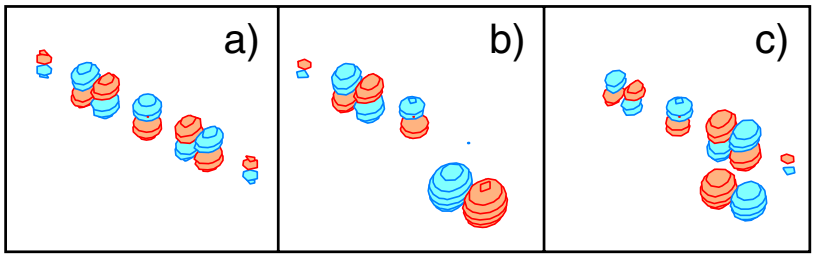

Figure 14.4: *Three selected molecular orbitals with dominant $3d_{zx}$ character on the coppers. The red regions indicate negative sign. a) undoped and $\Delta E_{0,zx} = -2.18$ eV. b) with Sr and $\Delta E_{0,zx} = -2.36$ eV. c) with Sr and $\Delta E_{0,zx} = -2.05$ eV. Note the substantially extended $2p_x$ orbital on the apex oxygen atom between the Cu and the Sr atom.*

number of rationalizations can be forwarded linking the origin to the proximity of the higher positive charge of the La^{3+} ion compared to the Sr^{2+} ion.

The additional splitting of the MOs in the right panel is due to different admixtures of $2p_z$ contributions from the apical oxygen that bridges the Cu site and the Sr. The MOs with $3d_{xy}$ character are not shown in Fig. 14.3 since they show no substantial difference between the doped and undoped clusters.

We thus find a rearrangement of the local electronic structure upon doping. This then involves a change in the spin-orbit contribution $A^{\alpha}_{\rm so}$ to the hyperfine field which will influence the nuclear spin-lattice relaxation times. We estimate an increase in A^{x}_{so} and A^{y}_{so} of about 15 to 20 %.

14.1.3 Local distortions in doped La_2CuO_4

In recent years, the experiments that probe the local structure have indicated the presence of significant local distortions in high-temperature superconductors. These structural deformations were attributed to the inhomogeneous charge distributions of a stripe phase. First clear evidence of this behaviour was obtained when Bianconi et al. [5] performed Cu K-edge extended x-ray absorption fine structure (EXAFS) on $La_{1.85}Sr_{0.15}CuO_4$. They found a bimodal length distribution for both Cu-O(ap) and Cu-O(pl) distances. In particular, an anomalously short Cu-O(ap) bond length of 2.30 Å was observed and attributed to the CuO_6 octahedra in the presence of an additional, extrinsic hole. This proposal was investigated in our recent first principles study [6] in which the distance between the copper and the apical oxygen, O(ap), was calculated for a cluster model with two different charge states: for a $(CuO_6)^{10-}$ ion (model A) and for a $(CuO_6)^{9-}$ ion (model A^+). Model A simulated the copper environment away from dopant ions, extrinsic holes, or any other defects, whereas model A^+ differed from model A by the presence of an additional extrinsic hole. It was assumed that the extrinsic-intrinsic hole pair for model A^+ forms a singlet state. The dependence of the energy as a function of the Cu-O(ap) distance is shown in Fig. 14.5. Note that the equilibrium O(ap)

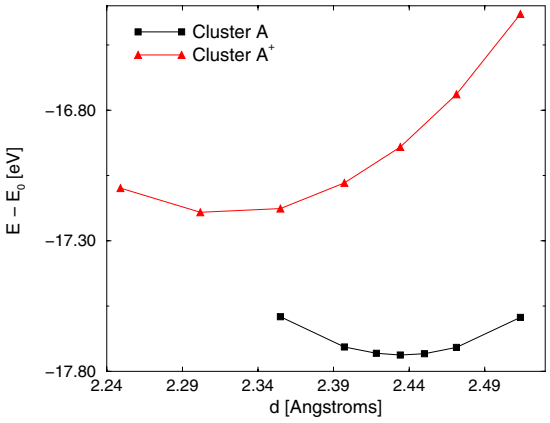

Figure 14.5: *Dependence of the ground-state energy on the Cu-O(ap) distance for model A and model A^+.*

location in cluster model A is shifted by $\delta_z = +0.04$ Å from the initial position at $z = 2.40$ Å which is attributed to the finite size of the cluster used. From Fig. 14.5 it can be seen that a localized hole induces a contraction of the Cu-O(ap) bond length by 0.12 Å which is in excellent agreement with the EXAFS investigation which obtain an anomalous Cu-O(ap) distance that was shortened by 0.1 Å with respect to the normal crystallographic distance of 2.40 Å as observed in the parent La_2CuO_4. The presented results of our study thus confirm the proposed interpretation for the observation of anomalous Cu-O(ap) distance in optimally doped La_2CuO_4.

14.2 Time series analysis of EEG

In the last decade, the time-series analysis of electroencephalograms (EEGs) by means of methods derived from nonlinear dynamics has attracted increased attention [7]. Traditionally the EEG is characterized mainly by linear properties such as the spectral power in certain frequency ranges. In contrast, nonlinear measures focussed in particular on the dimensional complexity (DC) [8], a measure based on the correlation dimension D_2. In this way a whole segment of an EEG is characterized by a single number. This amounts on the one hand to a strong data reduction, which is often very useful, and has on the other hand a plausible interpretation, i.e. the number of active degrees of freedom. The latter can also be interpreted as the degree of synchronization of the apparently high-dimensional neural dynamics. This interpretation is consistent with the estimates of the dimensional complexity in different psycho-physiological states from the EEG [9, 10] and the general ideas about the character of the neural dynamics in these states.

There is, however, clear evidence from the theory of nonlinear dynamics that the observed values of the dimensional complexity cannot simply be interpreted as dimensions of fractal attractors. Moreover, it was shown that surrogate time series of EEGs, i.e. time series, which resemble the linear properties of the original time series but are random otherwise, exhibit almost the same dimensional complexity as the original ones.

Starting from these findings we undertook a thorough investigation of the following two questions: Up to which extent does the dimensional complexity characterize only linear, i.e. spectral properties of the time series? And if so, which spectral properties are reflected in the dimensional complexity.

To demonstrate the simultaneous occurrence of both linear and nonlinear features in an EEG we investigated several all-night sleep EEGs. We obtained these data together with the sleep stage scores (REM, non-REM stages I, II, III, IV) from the Sleep Laboratory of the Institute of Pharmacology. We determined the correlation dimension D_2 using the Grassberger-Procaccia algorithm and the self-similarity exponent α by means of a detrended fluctuation analysis. The exponent α measures the persistence of a time series. Time series corresponding to values of α less than 1.5 have a tendency to turn back upon themselves. On the other hand, for α-values greater than 1.5, the time series has a tendency to be persistent in its progression in the direction in which it was moving. The latter property is known as persistence.

First, we analyzed 300 artifact-free EEG-segments of 1 minute duration, which were selected from four all-night sleep recordings, by applying the methods mentioned above. We divided the EEG-segments during sleep stage II into two subgroups: segments containing K-complexes and/or vertex waves were assigned to group II_B and those without such spikes to group II_A. In Fig. 14.6 we plotted the α-values on the ordinate against the D_2-values on the abscissa. It is seen that during REM sleep ($\bigcirc$) α is small and DC large. This is reversed during deep sleep (stages III/IV, $\triangle$). As concerns sleep stage II, the subgroup II_A follows the general trend between α and DC. The subgroup II_B, however, deviates. This indicates that the values of DC are much less affected by the occurrence of spikes in group II_B than the estimates of α. In general, it is evident that the α exponent can also distinguish different sleep stages. On the other hand, Fig. 14.6 makes clear that the α-values are negatively correlated with the estimated D_2.

Furthermore, we calculated DC and α for non-overlapping consecutive 1 minute long epochs from all-night sleep EEG-recordings. An inverse covariation between DC and α was detected as is seen in Fig. 14.7, where the variations of DC and α are plotted. One sees that both time variations reflect the cyclic changes in sleep dynamics which coincide with

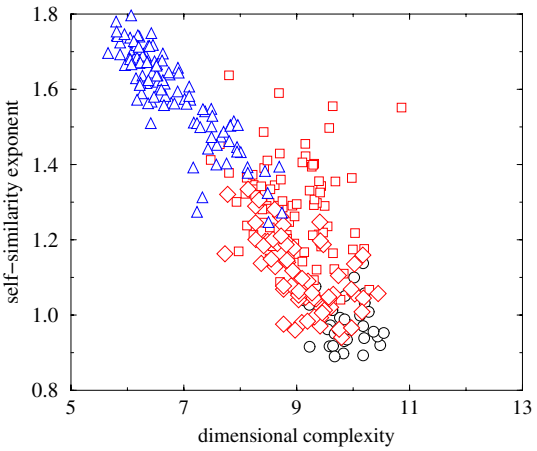

Figure 14.6: *Self-similarity exponent α vs. dimensional complexity D_2.*
△: sleep stage III/IV
◇: sleep stage group II_A
□: sleep stage group II_B
◯: REM sleep

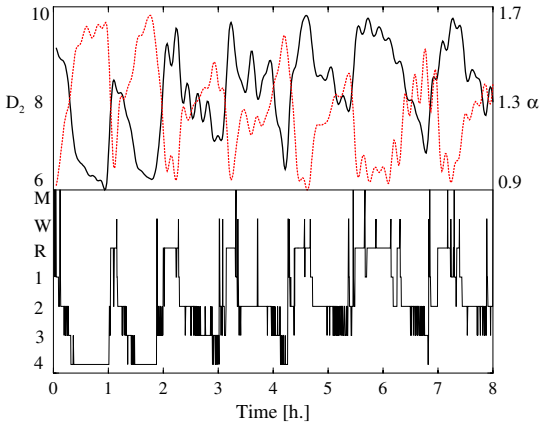

Figure 14.7: *The smoothed time courses of dimensional complexity D_2 (solid line in upper panel) and self-similarity α exponent (dotted line in upper panel) reflect the sleep stage scores (lower panel) and exhibit the inverse covariation.*

the sleep stage scores. The inverse covariation between DC and α and the fact that the DC-values of EEG-signals differ only slightly from those of surrogates led us to conclude that the DC measures mainly a linear property of EEG-signals – the persistence. Nevertheless, the deviations from this overall behaviour, as observed e.g. in sleep stage II, are valuable for further insights regarding the character of the EEG signals and will be the object of further research.

References

[1] Y. Zha, V. Barzykin, and D. Pines, Phys. Rev. B **54**, 7561 (1996).

[2] P. Hüsser, H. U. Suter, E. P. Stoll, and P. F. Meier, Phys. Rev. B **61**, 1567 (2000).

[3] E. P. Stoll, S. Pliberšek, S. Renold, T. A. Claxton, and P. F. Meier
J. Supercond. Inc. Nov. Magn. **13**, 971-975 (2000).

[4] S. Pliberšek and P. F. Meier, Europhys. Lett. **50**, 789 (2000).

[5] A. Bianconi et al., Phys. Rev. Lett. **76**, 3412 (1996).

[6] S. Pliberšek, E. P. Stoll, and P. F. Meier, Journal of Superconductivity **13**, 921 (2000).

[7] CHAOS IN BRAIN ?, edited by K. Lehnertz, J. Arnhold, P. Grassberger, and C.E. Elger, World Scientific, 1999.

[8] W. S. Pritchard and D. W. Duke, Int. J. Neuroscience **67**, 31 (1992).

[9] P. Achermann, R. Hartmann, A. Gunzinger, W. Guggenbühl, and A. A. Borbely, European Journal of Neuroscience **6**, 497 (1994).

[10] K. Lehnertz and C. E. Elger, Phys. Rev. Lett. **80**, 5019 (1998).